Polymorphic optical zoom with MEMS DMs

Yang Lu[1,*], Samuel M. Hoffman[1], Christopher R. Stockbridge[1], Andrew P. LeGendre[1], Jason B. Stewart[2], and Thomas G. Bifano[1]

[1]Photonics Center, Boston University, 8 Saint Mary's St., Boston, Massachusetts 02215
[2]Boston Micromachines Corporation, 30 Spinelli Pl., Cambridge, Massachusetts 02138
[*]Corresponding author: luyang@bu.edu

Abstract

A prototype optical system for compact, high-speed zooming is described. The system is enabled by a pair of MEMS deformable mirrors (DMs), and is capable of high-speed optical zoom without translation of components. We describe experiments conducted with the zoom system integrated with an optical microscope, demonstrating 2.5× zoom capability. Zoom is achieved by simultaneously adjusting focal lengths of the two DMs, which are inserted between an infinity-corrected microscope objective and a tube lens. In addition to zoom, the test system is demonstrated to be capable of automated fine focus control and adaptive aberration compensation. Image quality is measured using contrast modulation, and performance of the system is quantified.

Keywords: adaptive optics, deformable mirror, MEMS, polymorphic zoom

1. INTRODUCTION

The availability of compact, affordable deformable mirrors (DMs) makes it possible to explore alternatives to conventional optical configurations for zoom, focus, and aberration compensation. The proposed zoom approach trades component translation for component reshaping. We denote such DM-based zoom as "polymorphic" (literally: of many shapes) to differentiate it from conventional zoom lens assemblies that achieve zoom by mechanical translation of rigid components.

Various research groups have explored concepts similar to polymorphic zoom and active focusing in the past two decades. Much of that research has employed liquid lenses [1-5], spatial light modulators [6-8] or low-order membrane deformable mirrors [9-16] in proof-of-principle demonstrations. A general conclusion that can be drawn from this body of work is that when high-numerical apertures and off-axis beam paths are combined with active optics in an imaging system, the resulting images are often degraded by aberrations. Such aberrations have been characterized and found to be substantial for a number of specific active focusing configurations [10, 17, 18]. Recently, two systems with aberration-compensated optics were reported for active focusing [17] and active zoom [19]. One, developed at National Taiwan University, described a prototype autofocus module for consumer cameras that featured a MEMS DM and a rigid aspheric mirror that was intended to compensate expected off-axis aberrations. Observed image quality was poor and aberrations were not well compensated, but the system did establish a milestone as the first reported compact, active focus device with built-in aberration compensation. Another, currently in development at Fraunhofer, described a design for an all-reflective zoom. It also incorporated off-axis aspherical mirrors for aberration compensation. The design will use purely spherical DM shape control on initially curved DMs (which are not yet available). When completed, the DMs will be embedded in an optical zoom system that is statically aberration-compensated for a median zoom setting.

The system and approach described in this paper exploit the inherent capacity of existing DMs to compensate aberrations (in addition to changing component focal length), allowing broader flexibility in optical design. A brief introduction to active zoom and focus design, operation, and aberration compensation follows. Perhaps more importantly, the DM speed allows zooming at frame rates of up to 3kHz – far faster than that achievable with conventional zoom optics.

MEMS Adaptive Optics V, edited by Scot S. Olivier, Thomas G. Bifano, Joel A. Kubby, Proc. of SPIE
Vol. 7931, 79310D · © 2011 SPIE · CCC code: 0277-786X/11/$18 · doi: 10.1117/12.874207

2. MEMS DMS AND OPEN-LOOP CONTROLLABILITY

A pair of continuous face-sheet MEMS DMs with 140 electrostatic actuators (Boston Micromachines Corporation, MultiDM®) was used in this study. Each DM features 3.5μm stroke and 400μm pitch between actuators. The DMs are controlled in an open-loop fashion, using techniques developed previously by Diouf *et al* [20, 21]. Arbitrary shapes can be made with this control approach, with shape errors typically <25 nm rms. The images presented in Figure 1 qualitatively show the capability of this open-loop controller.

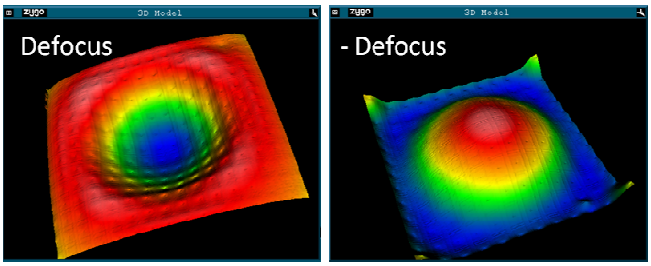

Figure 1: 2μm Peak-to-Valley DM defocus shapes made using open-loop controller, as measured with a surface mapping interferometer.

The relationship between central displacement of the DM, δ and mirror focal length f_{DM} is:

$$f_{DM} = \frac{D^2}{16\delta} \ , \tag{1}$$

where D is the diameter of the active aperture. In this work, we use an active optical aperture diameter of 3.6mm, incorporating 81 actuators. Actuators outside of the optical aperture are used to assist in open loop control, by minimizing mirror forces at the aperture edge. In the work reported here, we limit the DM open-loop shapes to those that produce central displacements less than ±2.5μm with respect to the aperture edge. With this constraint, the DM focal length can be varied from ±324mm to $\pm\infty$.

3. EXPERIMENTAL DEMONSTRATION

Optical Setup

A transparent, chrome-patterned 1951 USAF Resolution Target was used as a reference object for imaging experiments. It was imaged by a Nikon CF EPI 100×/0.95NA infinity-corrected objective using white light illumination.

The back pupil plane of the imaging objective was re-imaged to the first DM surface using a 4-f, unity-magnification telescope comprised of two 50mm focal-length lenses. The second DM was located 200mm from the first DM along the optical axis. A 200mm focal-length "tube" lens was located 50mm from the second DM and used to form the microscope image on a CCD camera (UNIQ UP-1830CL). Aperture stops measuring 3.6mm in diameter were located 30mm in front of each DM along the optical axis.

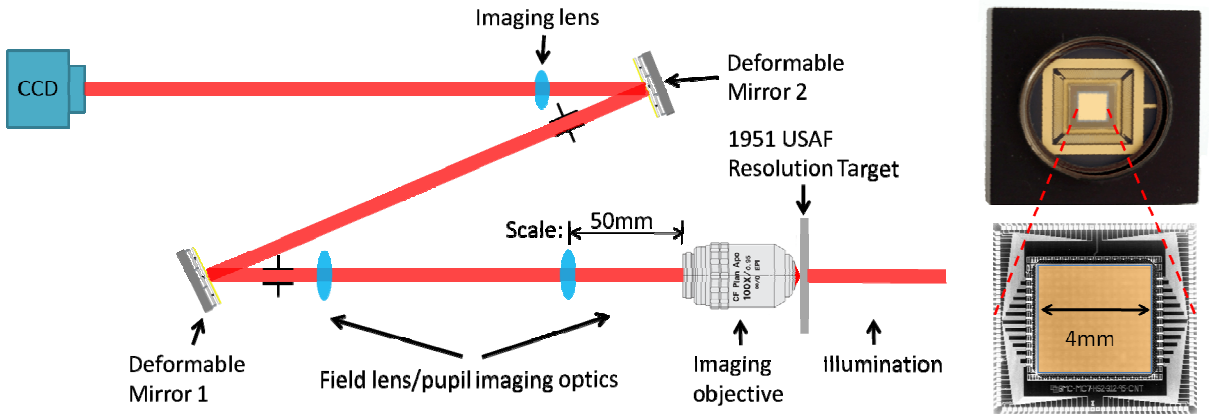

Figure 2: Left: Polymorphic zoom system schematic. Right: Optical microscope image of the deformable mirror.

Zoom Demonstration

The polymorphic zoom module, comprised of two DMs, is designed to be an afocal beam magnifier. It simply expands or contracts an incident collimated beam. Parallel rays entering the system will exit as parallel rays, though the spacing between rays will vary with magnification.

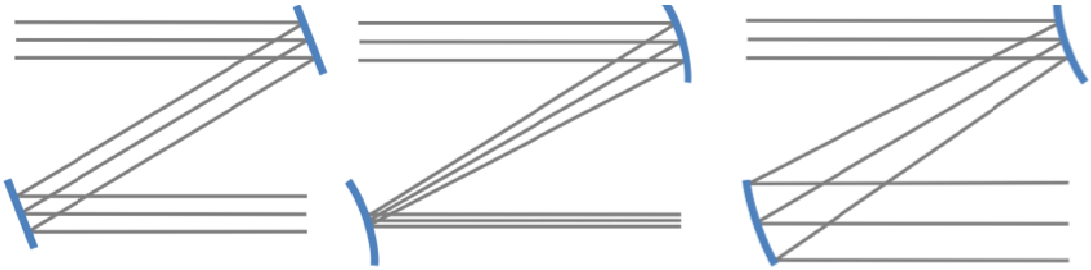

Figure 3: Polymorphic zoom module schematic. Left: When both DMs are flattened, the magnification is 1. Middle: When the first DM is concave (f>0), and the second DM collimates the beam, the magnification is <1. Right: When the first DM is convex (f<0), and the second DM collimates the beam, the magnification is >1.

Entering rays reflect from the first DM, travel in free space a distance s, and then reflect from the second DM. The ray optical propagation through the system can be modeled using matrix representation:

$$\begin{pmatrix} y' \\ \theta' \end{pmatrix} = \begin{pmatrix} 1 & 0 \\ -\frac{1}{f_2} & 1 \end{pmatrix} \begin{pmatrix} 1 & s \\ 0 & 1 \end{pmatrix} \begin{pmatrix} 1 & 0 \\ -\frac{1}{f_1} & 1 \end{pmatrix} \begin{pmatrix} y \\ \theta \end{pmatrix}, \tag{2}$$

$$y' = (1 - \frac{s}{f_1}) y + s\theta, \tag{3}$$

$$\theta' = (\frac{s}{f_1 f_2} - \frac{1}{f_1} - \frac{1}{f_2}) y + (1 - \frac{s}{f_2})\theta, \tag{4}$$

where y and y' are input position and output position with respect to the optical axis, and θ and θ' are the input angle and output angle with respect to the optical axis.

For an afocal zoom module, if $\theta = 0$ then $\theta' = 0$ for all y .Therefore, Equation (4) becomes:

$$(\frac{s}{f_1 f_2} - \frac{1}{f_1} - \frac{1}{f_2}) = 0 . \tag{5}$$

As a result, the operational constraint required afocal zoom is:

$$f_1 + f_2 = s . \tag{6}$$

Note that the magnification M and zoom ratio Z are:

$$M = -\frac{f_2}{f_1}, \tag{7}$$

$$Z = \frac{M_{\max}}{M_{\min}} . \tag{8}$$

Calculated magnifications for different focal lengths that satisfy Equation 6 are shown in Table 1.

Table 1: Magnification for afocal zoom with DMs separated by 200mm

f_{DM1} (mm)	-324	-500	-1000	∞	1000	700	524
f_{DM2} (mm)	524	700	1200	∞	-800	-500	-324
M	1.61	1.40	1.20	1.00	0.80	0.71	0.62

A maximum zoom of ~2.5× is achievable. The resulting images of a 1951 USAF Resolution Target, Group 9 (line spacing minimum ~1.5μm) are shown in Figure 3.

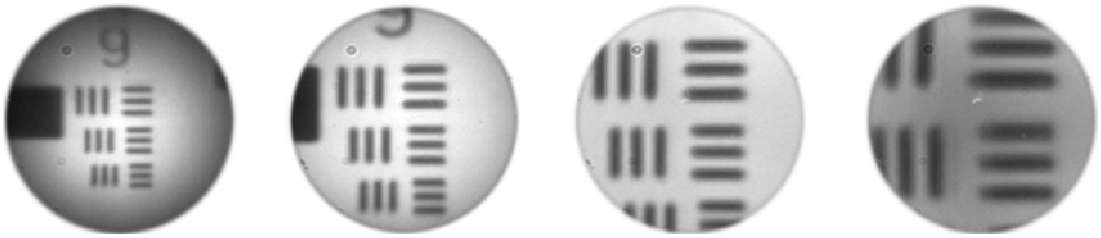

Figure 3: From left to right: 1× zoom, 1.5× zoom, 2× zoom, and 2.5× zoom.

Note that the image becomes dimmer for larger zoom settings. This is expected, since the expanding beam reflected from the first DM is clipped by the aperture stop in front of the second DM for large zoom settings.

Aberration Compensation

Since the objective is well-compensated, the aberrations due to optical imperfections are small in this experimental setup. Therefore, we manually translate the target 1μm away from the focal point to introduce an artificial defocus aberration for the demonstration of DM correction capability.

The combined effective focal length, f_{eff} , of the objective and the first DM is:

$$f_{eff} = \frac{f_{obj} f_{DM}}{f_{obj} + f_{DM}}, \tag{9}$$

where f_{obj} and f_{DM} are the focal lengths of the objective and the DM respectively.

If the 1951 USAF Resolution Target is translated along the optical axis by an amount Δ (at unity zoom ratio), the DM focal length can be adjusted to keep the combined system infinity-corrected. The specific requirement is that:

$$\Delta + f_{obj} = \frac{f_{obj} f_{DM}}{f_{obj} + f_{DM}}. \tag{10}$$

We can combine this with Equation (1) and ignore the f_{obj} term in the denominator, since the focal length of the objective is much smaller than any focal length achievable with the DM. The resulting relationship between object translation Δ and required DM central displacement δ can be expressed as follows:

$$\Delta = -\frac{16\delta f_{obj}^2}{D^2}. \tag{11}$$

As expected, DM defocus amplitude scales linearly with object translation.

For feedback control of imaging aberrations we used Contrast Transfer Function (CTF) to quantify contrast in an image subregion containing three bars of the target.

$$CTF = \frac{I_{\max} - I_{\min}}{I_{\max} + I_{\min}}. \tag{12}$$

We applied second and third order open-loop Zernike shapes (astigmatism, focus, trefoil, and coma) to the DM with amplitudes from -1μm to 1μm and used CTF as a feedback metric to perform aberration compensation. Each term was optimized independently and sequentially, in the following order: focus, astigmatism, trefoil, and coma. Each optimized Zernike shape was fixed and added by superposition to all subsequent higher order Zernike term optimization trials.

Figure 6 shows the results of open-loop Zernike shape compensation. The image quality, as measured by CTF, is improved by a factor of ~2 in comparison to the aberrated image. When more Zernike terms were added, we observed CTF improvement by ~10% in comparison to focus control alone.

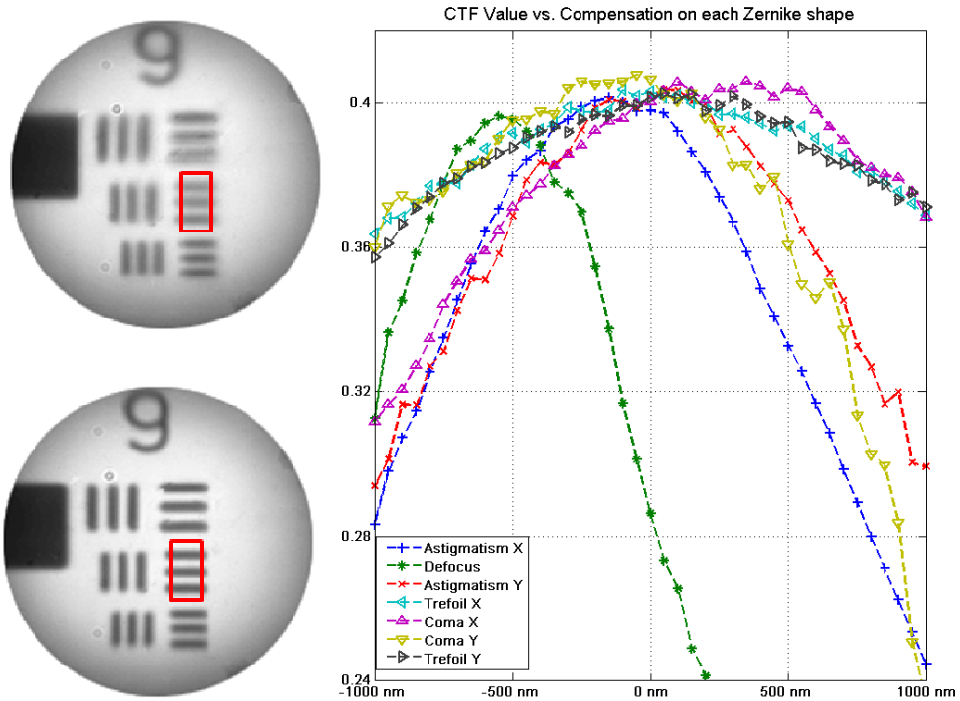

Zernike Term	Aberration Name	Shape PV(nm)	Shape RMS(nm)
3	Astigmatism X	-150	-31.4
4	Defocus	-550	-158.9
5	Astigmatism Y	-50	-10.6
6	Trefoil X	-100	-18.0
7	Coma X	100	18.0
8	Coma Y	-50	-9.0
9	Trefoil Y	50	9.0

Figure 6: Aberration compensation using open-loop Zernike scanning approach. Top left image: before/after correction. Top Right: CTF value vs. each Zernike shape. Bottom: compensation by terms

4. CONCLUSION

A polymorphic zoom system with 2.5× zoom and aberration compensation capability was demonstrated on a microscope, using a pair of MEMS DMs. Zoom capability depends on both DM separation and DM achievable stroke. Aberrations, misalignments, and off-axis beam paths were compensated using the first DM, which was conjugate to the objective back pupil plane of the microscope objective.

REFERENCES

[1] Feng G-H, Chou Y-C, "Flexible meniscus/biconvex lens system with fluidic-controlled tunable-focus applications," *Appl. Opt.*, [48], 3284-3290, (2009).

[2] Ren H, Wu S-T, "Variable-focus liquid lens," *Opt. Express*, [15], 5931-5936, (2007).

[3] Zhang D-Y, Justis N, Lo Y-H, "Integrated fluidic adaptive zoom lens," *Opt. Lett.*, [29], 2855-2857, (2004).

[4] Peng R, Chen J, Zhuang S, "Electrowetting-actuated zoom lens with spherical-interface liquid lenses," *J. Opt. Soc. Am. A*, [25], 2644-2650, (2008).

[5] Kuiper S, Hendriks BHW, "Variable-focus liquid lens for miniature cameras," *Applied Physics Letters*, [85], 1128-1130, (2004).

[6] Iemmi C, Campos J, "Anamorphic zoom system based on liquid crystal displays," *Journal of the European Optical Society*, [4], 09029, (2009).

[7] Tam EC, "Smart electro-optical zoom lens," *Opt. Lett.*, [17], 369-371, (1992).

[8] Park JH, Garipov GK, Jeon JA, Khrenov BA, Kim JE, Kim M, Kim YK, Lee CH, Lee J, Na GW, Nam S, Park IH, Park YS, "Obscura telescope with a MEMS micromirror array for space observation of transient luminous phenomena or fast-moving objects," *Opt. Express*, [16], 20249-20257, (2008).

[9] Wick DV, Martinez T, "Adaptive optical zoom," *Optical Engineering*, [43], 8-9, (2004).

[10] Dickensheets DL, "Requirements of MEMS membrane mirrors for focus adjustment and aberration correction in endoscopic confocal and optical coherence tomography imaging instruments," *Journal of Micro/Nanolithography, MEMS and MOEMS*, [7], 021008-021009, (2008).

[11] Bagwell BE, Wick DV, Cowan WD, Spahn OB, Sweatt WC, Martinez T, Restaino SR, Andrews JR, Wilcox CC, Payne DM, Romeo R, "Active zoom imaging for operationally responsive space," *SPIE MEMS Adaptive Optics*, San Jose, CA, USA, *SPIE*, [6467], 64670D-64678, (2007).

[12] Himmer PA, Dickensheets DL, Friholm RA, "Micromachined silicon nitride deformable mirrors for focus control," *Opt. Lett.*, [26], 1280-1282, (2001).

[13] Vdovin G, "Quick focusing of imaging optics using micromachined adaptive mirrors," *Optics Communications*, [140], 187-190, (1997).

[14] Wang J-L, Chen T-Y, Liu C, Chiu C-WE, Su G-DJ, "*Polymer Deformable Mirror for Optical Auto Focusing",* Electronics and Telecommunications Research Institute, Taejon, COREE, REPUBLIQUE DE, vol. 29, pp. 3,(2007)

[15] Martinez T, Wick DV, Payne DM, Baker JT, Restaino SR, "Non-mechanical zoom system," *Sensors, Systems, and Next-Generation Satellites VII*, Barcelona, Spain, *SPIE*, [5234], 375-378, (2004).

[16] Krogmann F, et al., "A MEMS-based variable micro-lens system," *Journal of Optics A: Pure and Applied*

Optics, [8], S330, (2006).
[17] Hsieh H-T, Wei H-C, Lin M-H, Hsu W-Y, Cheng Y-C, Su G-DJ, "Thin autofocus camera module by a large-stroke micromachined deformable mirror," *Opt. Express*, [18], 11097-11104, (2010).
[18] Mik A, Nov·k J, "Third-order aberrations of the thin refractive tunable-focus lens," *Opt. Lett.*, [35], 1031-1033, (2010).
[19] Seidl K, Knobbe J, Gr¸ger H, "Design of an all-reflective unobscured optical-power zoom objective," *Appl. Opt.*, [48], 4097-4107, (2009).
[20] Stewart JB, Diouf A, Zhou YP, Bifano TG, "Open-loop control of a MEMS deformable mirror for large-amplitude wavefront control," *Journal of the Optical Society of America a-Optics Image Science and Vision*, [24], 3827-3833, (2007).
[21] Diouf A, Bifano TG, Legendre AP, Lu Y, Stewart JB, "Open loop control on large stroke MEMS deformable mirrors," *MEMS Adaptive Optics IV*, San Francisco, California, USA, *SPIE*, [7595], 75950D-75957, (2010).